AGU PUBLICATIONS

Geophysical Research Letters

RESEARCH LETTER
10.1002/2017GL076446

Special Section:
The Arctic: An AGU Joint Special Collection

Collapse of the 2017 Winter Beaufort High: A Response to Thinning Sea Ice?

G. W. K. Moore[1,2], A. Schweiger[3], J. Zhang[3], and M. Steele[3]

[1]Department of Physics, University of Toronto, Toronto, Ontario, Canada, [2]Jackson School of International Studies, University of Washington, Seattle, WA, USA, [3]Polar Science Center, Applied Physics Laboratory, University of Washington, Seattle, WA, USA

Key Points:
- The extreme warmth during the autumn of 2016 resulted in reduced sea ice cover in the eastern Arctic that persisted into the winter of 2017
- The resulting enhanced air-sea interaction allowed extratropical cyclones from the North Atlantic to intrude into the western Arctic
- This leads to the collapse of the Beaufort High resulting in a reversal in surface winds and sea ice motion across the entire western Arctic

Supporting Information:
- Supporting Information S1

Correspondence to:
G. W. K. Moore,
gwk.moore@utoronto.ca

Citation:
Moore, G. W. K., Schweiger, A., Zhang, J., & Steele, M. (2018). Collapse of the 2017 winter Beaufort High: A response to thinning sea ice? *Geophysical Research Letters*, *45*, 2860–2869. https://doi.org/10.1002/2017GL076446

Received 16 NOV 2017
Accepted 19 FEB 2018
Accepted article online 19 MAR 2018
Published online 26 MAR 2018

Abstract The winter Arctic atmosphere is under the influence of two very different circulation systems: extratropical cyclones travel along the primary North Atlantic storm track from Iceland toward the eastern Arctic, while the western Arctic is characterized by a quasi-stationary region of high pressure known as the Beaufort High. The winter (January through March) of 2017 featured an anomalous reversal of the normally anticyclonic surface winds and sea ice motion in the western Arctic. This reversal can be traced to a collapse of the Beaufort High as the result of the intrusion of low-pressure systems from the North Atlantic, along the East Siberian Coast, into the Arctic Basin. Thin sea ice as the result of an extremely warm autumn (October through December) of 2016 contributed to the formation of an anomalous thermal low over the Barents Sea that, along with a northward shift of the tropospheric polar vortex, permitted this intrusion. The collapse of the Beaufort High during the winter of 2017 was associated with simultaneous 2-sigma sea level pressure, surface wind, and sea ice circulation anomalies in the western Arctic. As the Arctic sea ice continues to thin, such reversals may become more common and impact ocean circulation, sea ice, and biology.

Plain Language Summary The warming that the Arctic is currently experiencing has garnered attention in both the popular and scientific press. Indeed, the retreat and thinning of the region's sea ice is one of the most significant and irrefutable indicators of human influence on the climate. In addition to these long-term trends, the past several years have seen record warmth and extreme events in the region, such as above-freezing winter temperatures at the North Pole, which may be harbingers of even more dramatic changes in the future. In this paper, we document a recent and previously unknown consequence of this warming: the collapse of the winter Beaufort High that occurred as a result of the intrusion of North Atlantic cyclones into the western Arctic. This phenomenon occurred, for the first time, during the winter of 2017 and resulted in a reversal in surface winds and sea ice motion across the entire western Arctic. We argue that the extreme warmth during the autumn of 2016 resulted in reduced sea ice extent and thickness in the eastern Arctic that persisted into the winter of 2017 allowing extratropical cyclones from the North Atlantic to intrude into the western Arctic.

1. Introduction

The winter Arctic atmosphere is under the influence of two very different circulation systems. The eastern Arctic is impacted by extratropical cyclones that travel from Iceland toward the Barents Sea along the primary North Atlantic storm track (Hoskins & Hodges, 2002; Serreze et al., 1997). A signature of this storm track is the trough in sea level pressure (SLP) that extends northeastward from the Icelandic Low (Moore et al., 2012). Often, this trough has a closed secondary circulation center over the Norwegian Sea that is referred to as the Lofoten Low (Jahnke-Bornemann & Brummer, 2009). In contrast, the circulation in the western Arctic is characterized by a quasi-stationary region of high pressure known as the Beaufort High (Walsh, 1978). Although it is usually connected to the Siberian High through a ridge of high pressure, the Beaufort High is normally a closed anticyclone during the winter (Serreze & Barrett, 2010).

The gradient in the winter surface air temperature (SAT) between the eastern and western Arctic (Moore, 2016; Serreze & Barry, 2014) is also indicative of the differences in these two circulation systems. The eastern Arctic tends to be warmer as a result of the poleward advection of heat by the cyclones that travel along the primary North Atlantic storm track (Serreze & Barry, 2005). Local oceanic heat loss that occurs during cold air outbreaks over the Nordic Seas (Brummer, 1999) has been argued to be an important contributor to this

transport (Tsukernik et al., 2007). In contrast, the combination of the Siberian and Beaufort Highs tends to advect cold and dry continental air from Eurasia into the western Arctic (Serreze & Barrett, 2010).

The Beaufort High forces the oceanic Beaufort Gyre (McPhee, 2012; Proshutinsky et al., 2009) and anticyclonic sea ice motion that plays a role in the sea ice mass balance of the Arctic Ocean (Rigor et al., 2002). Over the last two decades, the Beaufort Gyre has accumulated significant amounts of fresh water as a result of this anticyclonic forcing (Haine et al., 2015). In addition, a recent amplification of sea ice motion in the Beaufort Sea has been noted that was proposed to be the result of enhanced wind forcing and thinner and more mobile ice pack (Petty et al., 2016).

Arctic sea ice has been declining since 1979 (Stroeve et al., 2012). This loss of sea ice is most pronounced during the summer (Cohen et al., 2014; Parkinson & Cavalieri, 2008), leading to enhanced warming of the ocean surface (Steele et al., 2008). There has also been a winter loss of sea ice cover focused mainly in the Greenland, Iceland, and Barents Seas (Arthun et al., 2012; Moore et al., 2015) and an overall thinning of sea ice with reduced ice volume and increased ice mobility and lead opening (Lindsay & Zhang, 2005; Zhang et al., 2012).

During December 2015, the SAT at the North Pole rose above freezing, generating much discussion (Batty, 2015; Boisvert et al., 2016; Moore, 2016). This transient warming event was associated with a deep extratropical cyclone that traveled northward from the Greenland Sea, transporting heat and moisture into the North Pole region (Moore, 2016). This unusual warmth continued through winter of 2016, with a split polar vortex that led to anomalous northward transport into the western Arctic and over central Eurasia (Cullather et al., 2016; Overland & Wang, 2016).

Our focus here is on the winter of 2017. This season was also warm in the Arctic, but not as warm of 2016. However, what distinguished it was a complete reversal of the normally anticyclonic sea ice motion in the western Arctic. We will show that this reversal of sea ice motion can be traced to a collapse of the Beaufort High as a result of the intrusion of low-pressure systems from the North Atlantic, along the East Siberian Coast, far into the Arctic Basin. We argue that extreme warmth during the autumn of 2016 contributed to this reversal through reduction in sea ice thickness that persisted into the following season as did anomalous upper tropospheric forcing and reduced lower tropospheric stratification.

2. Data and Methods

We analyze surface and upper air fields from the ERA-I Reanalysis (Dee et al., 2011). The data are available at a ~75 km horizontal and 6-hourly temporal resolution (Dee et al., 2011). Numerous studies have confirmed the ability of the ERA-I Reanalysis to represent the spatial and temporal variability of the Arctic surface and upper atmospheric circulation (Bromwich et al., 2016; Lindsay et al., 2014; Moore, 2016). To track the passage of cyclones and their influence, we employ an Eulerian diagnostic based on a 2–6 day band-pass filter of the variance in the SLP field (Blackmon et al., 1977). Regions with elevated values of this field provide an indicator of enhanced storm track activity (Chang, 2009). Please refer to the supporting information for additional information on this diagnostic.

For a longer-term perspective on Arctic SAT variability, we will use the NASA GISS Surface Temperature Analysis (GISTEMP) (Hansen et al., 2010). To address the scarcity of Arctic observations during the early part of the instrumental record, the GISTEMP data set uses spatial interpolation that acts to reduce the uncertainty in the regional SATs (Chylek et al., 2010; Hansen et al., 1999). As an additional check, the HADCRUT4 SAT data set (Morice et al., 2012), which does not do any spatial interpolation, was also used.

Analysis of sea ice conditions is based on NASA Team data set, for sea ice concentration (Cavalieri et al., 1999), and the Pan-Arctic Ice Ocean Modeling and Assimilation System (PIOMAS) for sea ice thickness and motion (Zhang & Rothrock, 2003). PIOMAS assimilates satellite sea ice concentration and sea surface temperature and is calibrated and validated with a variety of sea ice thickness observations (Schweiger et al., 2011; Zhang & Rothrock, 2003). Sea ice motion in PIOMAS is calibrated and validated by the International Arctic Buoy Program (IABP (Rigor et al., 2002)) sea ice drift data (Schweiger & Zhang, 2015; Zhang et al., 2012). PIOMAS is forced by the NCEP/NCAR Reanalysis atmospheric data.

Details on Arctic Ocean sea surface temperatures (SST) are provided by NOAA's Optimum Interpolation Sea Surface Temperature (OISST) data set, a global, daily mean product with 0.25° spatial resolution

(Banzon et al., 2016). We use the version derived from a blend of in situ observations and Advanced Very High Resolution Radiometer (AVHRR) infrared sensors, which provides a consistent multiyear time series over the years 1982 to present. Please refer to the supporting information for additional information on this data set.

We will focus on the time period from 1979 onward, with analysis extending back to 1900 providing a longer-term context. We define as autumn as the months of October through December (OND) and winter as the months of January through March (JFM).

3. Results

Figure S1 shows Arctic regional mean SAT time series during both the autumn and the winter over the period 1979–2017. Also shown is the low-frequency behavior using Singular Spectrum Analysis technique (Ghil et al., 2002) and a measure of interannual variability that takes this behavior into account. This figure shows the accelerated warming that has occurred in the Arctic since the 1990s (Serreze et al., 2009) and the recent extreme warmth. Indeed, the autumn of 2016 was the warmest since 1979, exceeding a two standard deviation threshold. We find similar results with the GISTEMP SAT data set over a longer time period (Figure S2), with the warming at high northern latitudes generally enhanced relative to global and Northern Hemisphere mean temperatures. Similar results were obtained with the HADCRUT4 SAT data set (not shown) that reflects the high degree of correlation, $r \sim 0.9$, between the GISTEMP and HADCRUT4 Arctic SAT over the period 1900–2017.

The autumn of 2015 sea surface temperature (SST) anomalies (Figure S3a) were generally small. On the other hand, the autumn of 2016 SST anomalies (Figure S3b) and also in Petty et al. (2017) were large and extensive throughout the Barents Sea. September 2016 SST anomalies (not shown) were generally small, indicating that autumn 2016 SST anomalies likely arose not from enhanced oceanic transport into the region but rather from suppression of ocean-to-atmosphere heat loss, probably owing to anomalously warm SAT that occurred during the season.

Despite its lack of record warmth, the winter of 2017 was nevertheless remarkable for an atmospheric circulation anomaly that developed in the western Arctic. Figure 1 shows tracks of IABP buoys (Rigor et al., 2002) during the winters of 2016 and 2017, as well as the corresponding SLP field from the ERA-I Reanalysis. Winter ice drift in 2016 was representative of climatological conditions (Rigor et al., 2002), with a well-defined Beaufort High associated with an anticyclonic sea ice gyre (i.e., eastward flow to the north of the high and westward flow to its south along the Alaskan coast). However, the winter of 2017 was very different, with eastward (i.e., cyclonic) sea ice motion throughout the region associated with a trough of low SLP extending into region from the eastern Arctic.

Figure 2 compares and contrasts the PIOMAS climatological sea ice motion and thickness with conditions during the winter of 2017. The climatological ice motion and that during 2017 are consistent with IABP buoy motion (Figure 1). Sea ice thickness was reduced during the winter of 2017, notably along the Siberian and Canadian Arctic Archipelago coasts, with dipoles occurring across the New Siberian and Wrangel Islands. These sea ice thickness changes are consistent with the observed reversal of sea ice motion in 2017; that is, sea ice was advected away from the Siberian coast and against Banks Island in the Beaufort Sea. The winter 2017 sea ice thickness anomaly relative to long-term climatology also includes the impacts of the long-term trend toward thinner sea ice (Schweiger et al., 2011), but similar results hold for a comparison between 2016 and 2017 as well (not shown).

The ERA-I Reanalysis (Figure 3a) shows climatological mean winter atmospheric conditions, with anticyclonic surface winds across the western Arctic, associated with the Beaufort High, and in the eastern Arctic, the Icelandic Low with its trailing trough extending northeastward toward the Barents Sea. As discussed above, this trough assists in the advection of warm midlatitude air up into the eastern Arctic and helps establish the observed SAT gradient between the eastern and western Arctic seen in Figure 3a. During the winter of 2017 (Figure 3b), in addition to the Icelandic Low, a separate low-pressure center developed over the Barents Sea, with a central pressure approximately 8 mb deeper than climatological SLP in this region. Anomalously large surface heating in the region of reduced ice cover (Figure S4) contributed to the formation of this thermal low. Please refer to the supporting information for additional information on the characterization of the surface heating. There was a trailing trough extending into the central Arctic associated with this

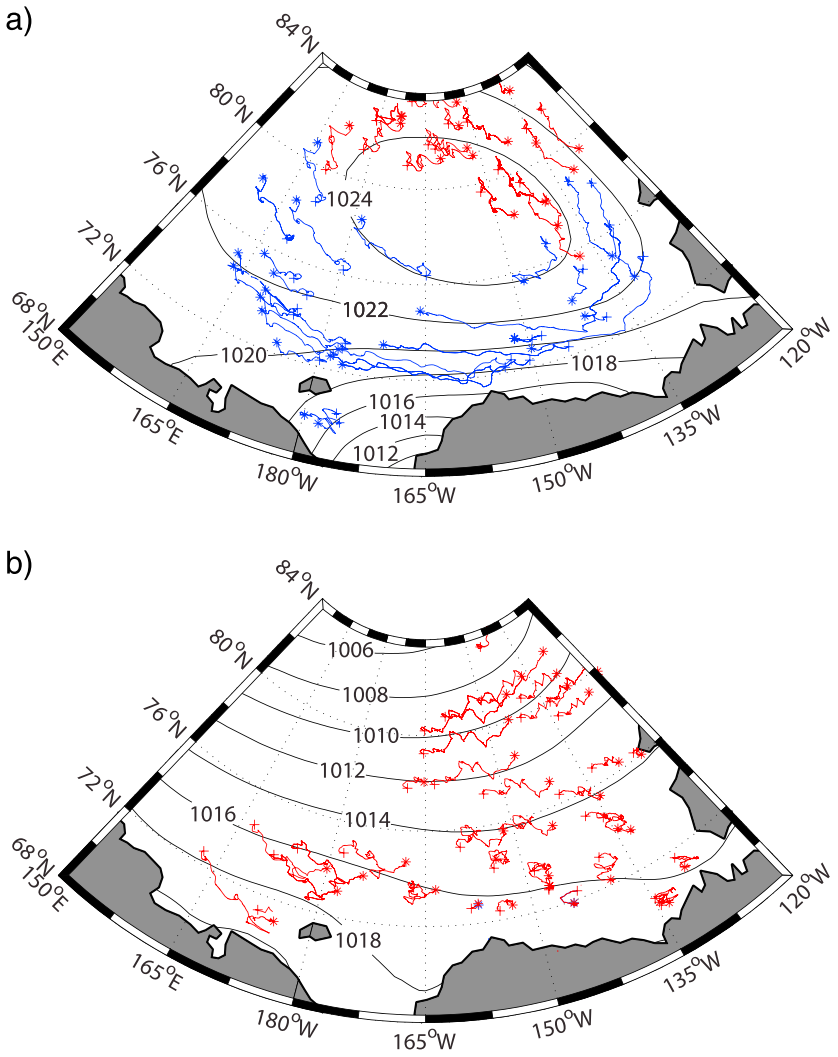

Figure 1. Buoy tracks in the western Arctic from the IABP during the winter (JFM) of (a) 2016 and (b) 2017. Eastward tracks are in red, and westward tracks are in blue with the "+" indicating the start of the track and the "*" the end of the track. Also shown is the corresponding SLP field (mb) from the ERA-I Reanalysis.

secondary low that resulted in anomalous sea ice drift across the western Arctic during the winter of 2017 (Figures 1b and 2b).

This Arctic trough ultimately resulted in the collapse of the Beaufort High and the southward retreat of the Siberian High. To support this connection, we consider the 2–6 day band-pass filtered SLP field that is an Eulerian diagnostic for storm track activity (Blackmon et al., 1977). During a typical winter (Figure 3c), the main North Atlantic storm track (Hoskins & Hodges, 2002) is seen as a region of high variance extending northeastward from Iceland to the Barents Sea, but no farther. Remarkably, a second distinct area of high variance in the Barents Sea developed during the winter of 2017 (Figure 3d), collocated with the thermal low-pressure center noted above, and extending westward along the Siberian coast and into the western Arctic. It is the signature of the anomalous intrusion of cyclones from the North Atlantic that occurred during the winter of 2017 and that resulted in the collapse of the Beaufort High. In the climatology, the Siberian coast is a region of low variance, associated with the quasi-stationary high pressures of the Beaufort and Siberian Highs.

Figure 4 shows time series of the SLP in the vicinity of the climatological center of the winter Beaufort High, the zonal component of the surface wind along the coast of the Beaufort and Chukchi Seas, both from the ERA-I Reanalysis and the curl of sea ice motion in the central Beaufort Sea from the PIOMAS Reanalysis. Positive/negative values of the latter parameter reflect cyclonic/anticyclonic sea ice motion. The domains

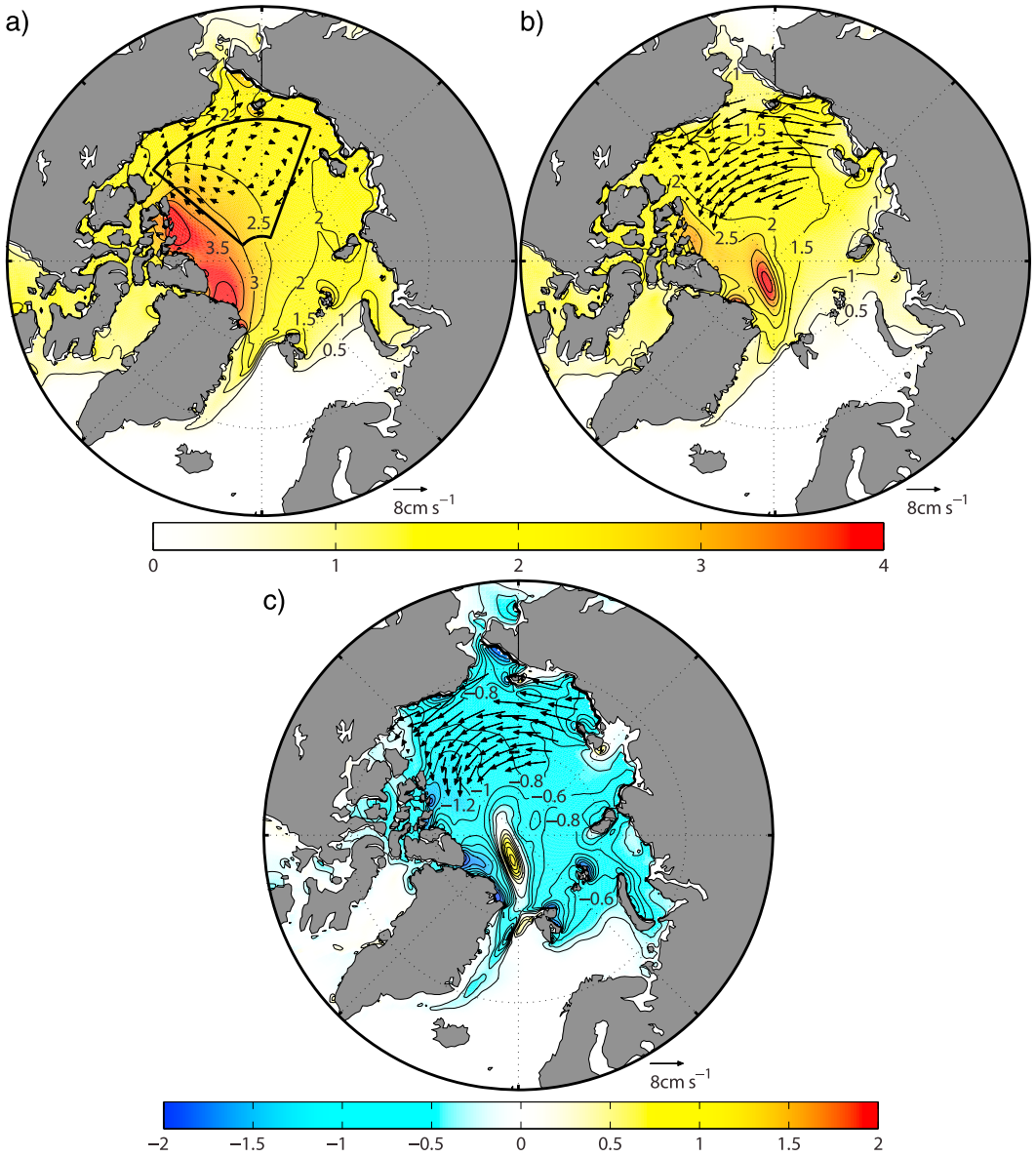

Figure 2. Sea ice conditions in the Arctic during the winter (JFM) from the PIOMAS Reanalysis 1979–2017. Thickness of the sea ice (contours and shading, m) and sea ice motion (vectors, cm/s) at selected grid points for (a) the climatological winter mean, (b) the 2017 winter mean, and (c) the difference between the winter of 2017 and the climatological winter mean. The domain over which the curl of the sea ice motion is averaged to generate the time series shown in Figure 4 is indicated in (a).

used to define these indices are indicated in Figures 2 and 3. While some winters can be characterized by anomalous values of one or two of these indices, the winter of 2017 is exceptional in that all three indices are in excess of two standard deviations above or below their respective long-term means.

The changes described above were also impacted by an unusual upper level atmospheric circulation pattern. During a typical winter, cyclonic flow in the upper troposphere is centered over the Canadian Arctic Archipelago (Cavallo & Hakim, 2010) with high values of potential vorticity on the 300 mb pressure surface in this region (Figure 5a). During the winter of 2017, this so-called tropospheric polar vortex shifted northward and intensified relative to climatology (Figure 5b). The interaction between the tropospheric polar vortex and the surface circulation feature is enhanced in regions of low tropospheric static stability, that is, regions with reduced vertical temperature gradients that can occur due to surface heating, since this increases the penetration depth of upper level circulation anomalies (Moore et al., 1996). Figure 5 also

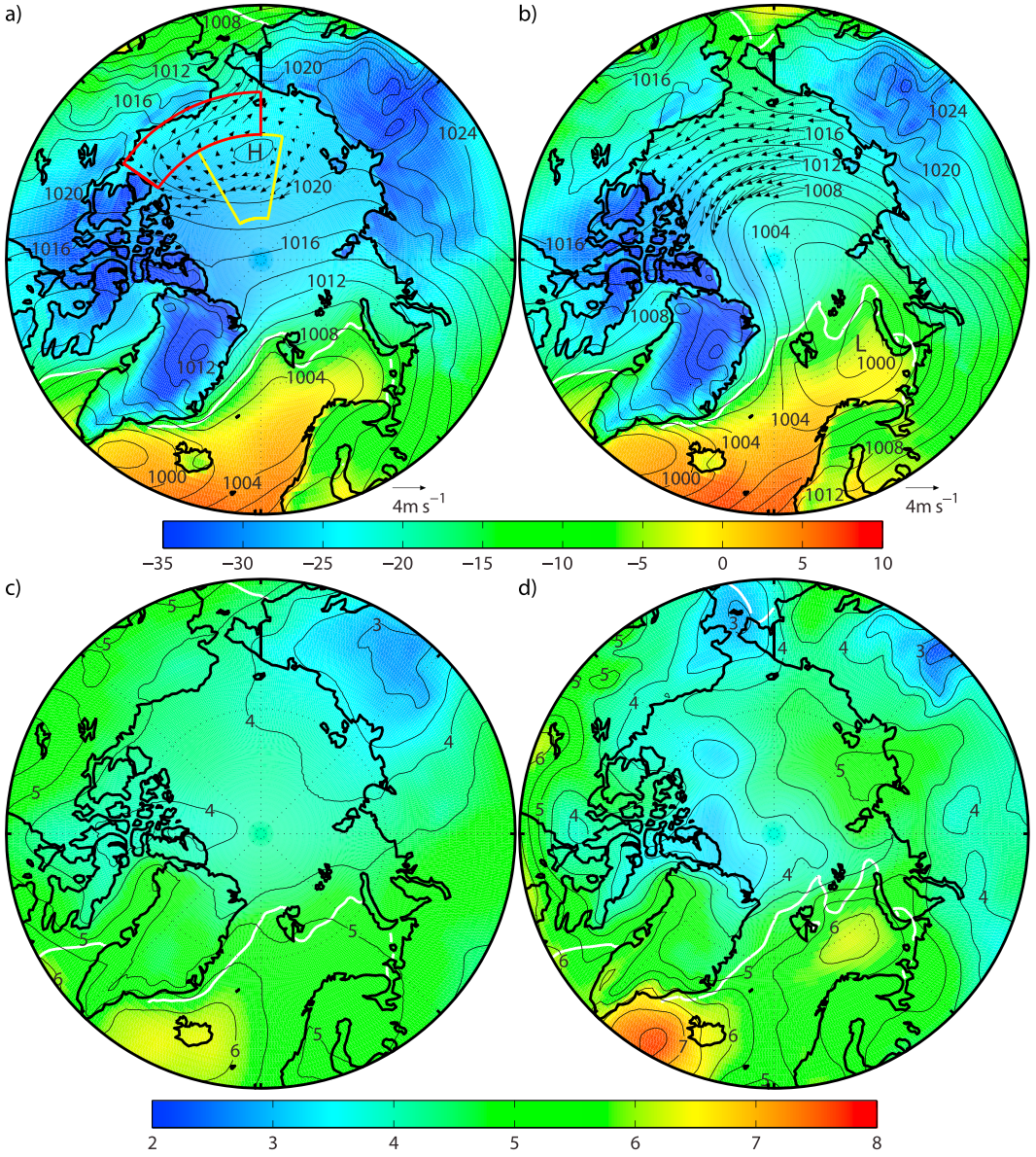

Figure 3. Surface environmental conditions in the Arctic during the winter (JFM) from the ERAI-Reanalysis 1979–2017. Sea level pressure (contours, mb), 2 m air temperature (shading, °C), and 10 m wind (vectors, m/s) at selected grid points for (a) the climatological winter mean and (b) the 2017 winter mean. The 2–6 day band-pass filtered variance of the sea level pressure (shading and contours, mb) for (c) the climatological winter mean and (d) the 2017 winter mean. In all panels, the white contour represents the 50% seasonal mean sea ice isocontour. In (a), the location of the climatological Beaufort High is indicated by the "H." In (b), the location of the anomalous thermal low is indicated by the "L." The domains over which the sea level pressure (yellow polygon) and the zonal component of the 10 m wind (red polygon) are averaged to generate the time series shown in Figure 4 are indicated in (a).

shows that tropospheric static stability throughout the Arctic was reduced during the winter of 2017 as compared to climatology. This reduction would have contributed to the coupling with the upper level circulation anomaly. The westward tilt with height of the surface and upper tropospheric circulation anomalies is also indicative of baroclinic processes contributing to cyclogenesis (Hoskinset al., 1985).

4. Discussion

The Arctic atmospheric circulation during the winter is typically characterized by high SLP in the western Arctic associated with the Beaufort and Siberian Highs (Serreze & Barrett, 2010) and low SLP in the eastern

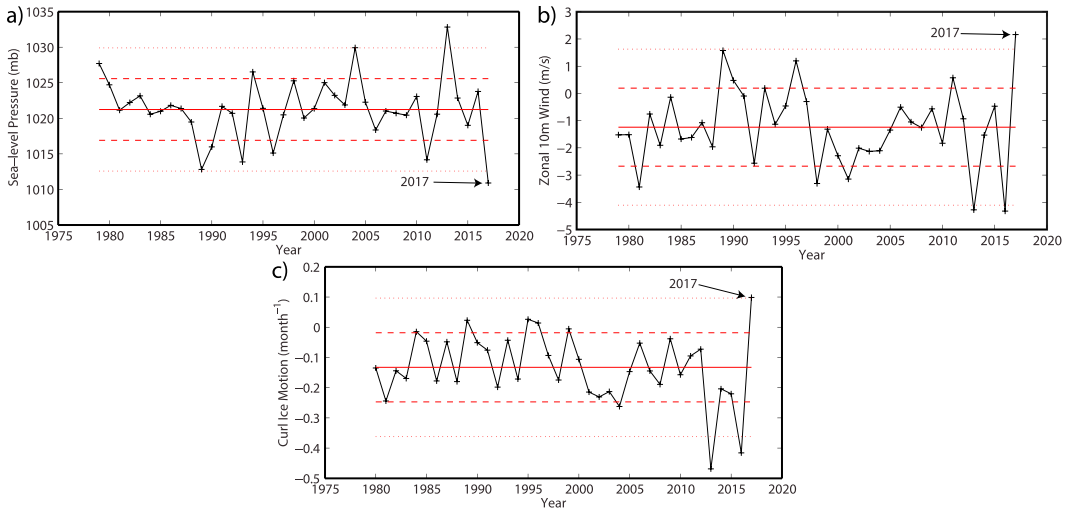

Figure 4. Time series of the winter mean (JFM): (a) SLP (mb) in the vicinity of the climatological center of the winter Beaufort High from the ERA-I Reanalysis 1979–2017, (b) the zonal wind (m/s) along the coast of the Chukchi and Beaufort Seas from the ERA-I Reanalysis 1979–2017, and (c) the curl of the sea ice motion (month^{-1}) in the central Beaufort Sea from the PIOMAS Reanalysis 1979–2017. The means are indicated by the red lines with one and two standard deviations above/below the mean indicated by the dashed and dotted lines.

Arctic that is the result of extratropical cyclones traveling along the primary North Atlantic storm toward the Barents Sea (Jahnke-Bornemann & Brummer, 2009; Moore et al., 2012). Both of these circulation systems play important roles in the climate system. For example, the surface wind associated with the winter Beaufort High drives the oceanic Beaufort Gyre and anticyclonic sea ice motion over the Beaufort Sea (Proshutinsky et al., 2009; Rigor et al., 2002). The cyclones that track from Iceland toward the Barents Sea contribute to the poleward heat transport into the eastern Arctic (Serreze & Barry, 2014).

Recent winters have been notable for the warmth driven by Arctic Amplification (Serreze et al., 2009) with 2016 holding the current record. The winter of 2017 was also warm but was particularly noteworthy for the reversal of the surface winds and sea ice motion in the western Arctic from their normally anticyclonic direction (Figures 1–3). This reversal was characterized by SLP, zonal wind, and sea ice circulation anomalies that all exceeded the 2-sigma threshold (Figure 4). Transient reversals have been noted previously (Asplin et al., 2009), but Figure 4 indicates that such a reversal has not previously occurred during an entire winter.

We propose that the reversal was caused by a collapse of the Beaufort High and a southward retreat of the Siberian High (Figure 3). We argue that warm SATs across the Arctic during the autumn of 2016 (Figures S1 and S2) resulted in reduced sea ice thickness that persisted into the subsequent winter (Figure 2). The resulting enhanced transfer of heat from the ocean to the atmosphere in the eastern Arctic provided an additional energy source for extratropical cyclones entering the region and contributed to the development of a thermal low over the Barents Sea (Figures 3b and S4). This circulation center may represent an extreme northward displacement of the Lofoten Low (Jahnke-Bornemann & Brummer, 2009).

This surface forcing in concert with the anomalous upper level circulation (Figure 5) created conditions permitting the intrusion of North Atlantic cyclones deep into the central Arctic (Figure 3d). This series of cyclones led to a reduction in SLP over the Beaufort Sea and the highly anomalous sea ice circulation over the western Arctic Ocean. Our analysis of the upper level circulation, lower tropospheric stability, and sea ice conditions suggests this as the primary mechanism leading to the reversal of the winds and sea ice motion in the western Arctic.

Model studies have examined the response of the Arctic atmosphere to the thinning and loss of sea ice (Deseret al., 2007; Semmleret al., 2016). These studies indicate that there is a transient response in which there is a reduction in SLP, most likely in response to the enhanced surface heating, which lasts for at most a few weeks. After this, a larger amplitude quasi-steady equilibrium state is reached that is characterized by a

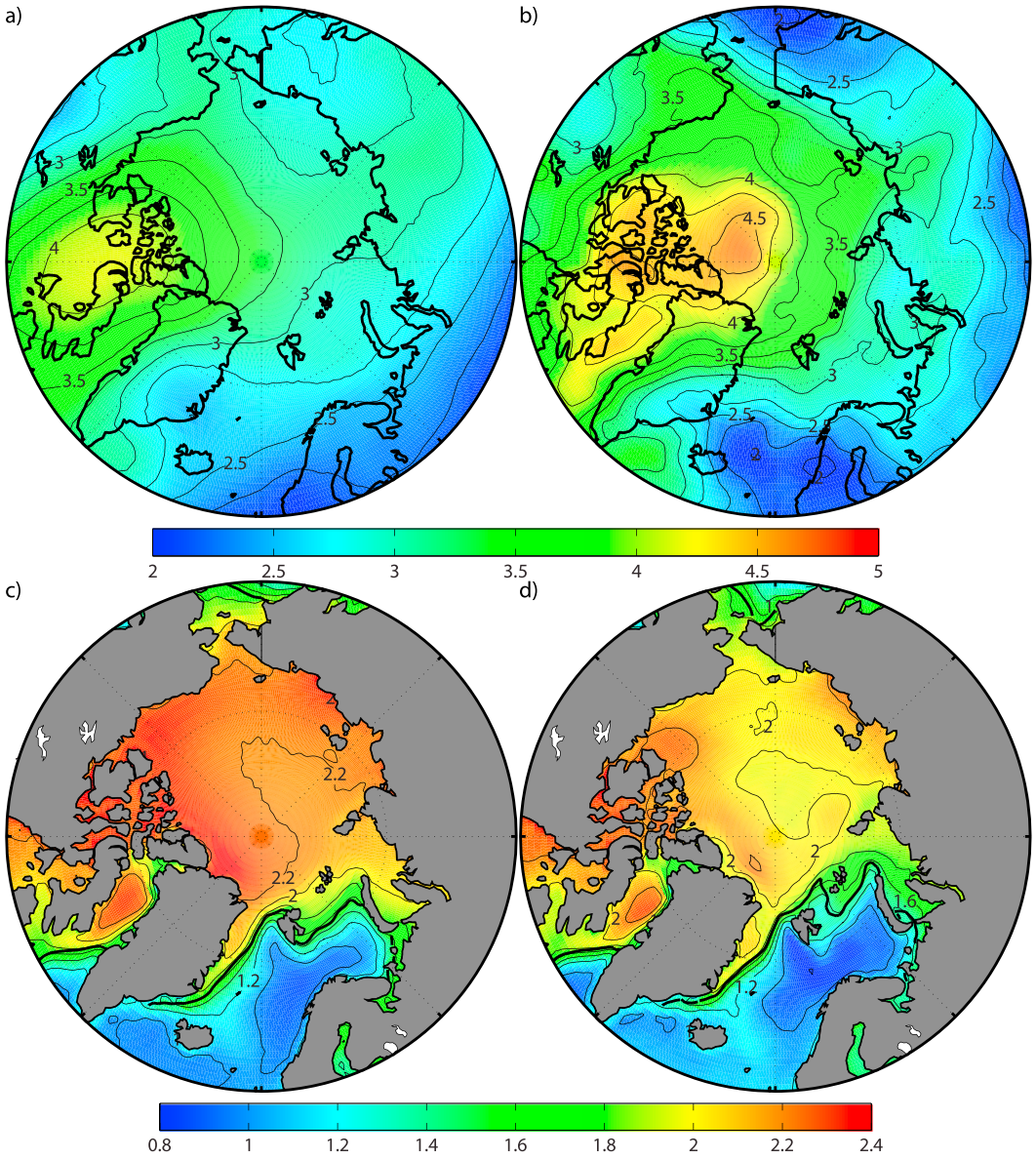

Figure 5. Tropospheric environmental conditions in the Arctic during the winter (JFM) from the ERAI-Reanalysis 1979–2017. The 300 mb potential vorticity (contours and shading, PVU) for (a) the climatological winter mean and (b) the 2017 winter mean. The 1000–700 mb Brunt-Väisälä frequency (s^{-1}) for (c) the climatological winter mean and (d) the 2017 winter mean. In panels (c) and (d), the thick black contour represents the 50% seasonal mean sea ice isocontour.

barotropic anticyclonic circulation that extends throughout the troposphere. Other studies show a reduction in Arctic cyclones during the winter in response to sea ice loss (Dayet al., 2017).

The conditions during the winter of 2017 were substantially different from these model results, with cyclonic flow at both the surface and at upper levels. Such model results typically focus on the mean response to changing sea ice conditions. This may mask the unique interactions between the upper level flow and the surface that lead to enhanced cyclogenesis, intrusion of cyclones into the central Arctic during winter, and the unprecedented winter reversal in sea ice motion. In addition, climate models do not yet accurately characterize the winter time storm tracks reaching from the North Atlantic into the Arctic (Day et al., 2017).

As Arctic sea ice continues to thin, more frequent pan-Arctic intrusions of North Atlantic cyclones are likely with concomitant implications for the Beaufort High and the climate of the region. For example, a

modeling study indicates that a weakening of this anticyclonic forcing (Manucharyan & Spall, 2016) can lead to a release of fresh water with potential impacts downstream on the salinity budget of the subpolar North Atlantic (Haine et al., 2015). In addition, given the role that the Beaufort High plays in sea ice transport (Rigor et al., 2002), its collapse would have significant implications on this transport.

Acknowledgments
The authors thank the reviewers for their comments. G. W. K. M. would like to acknowledge the support of the Canada Fulbright Foundation and the Jackson School of International Studies at the University of Washington and the Natural Sciences and Engineering Research Council of Canada. A. S. was supported by ONR grant N00014-17-1-3162, NSF grant ARC-1203425, and NOAA grant NA15OAR4310162. J. Z. was supported by NASA grants NNX17AD27G and NNX15AG68G, ONR grant N00014-12-1-0112, and NSF grants PLR-1416920 and PLR-1603259. M. S. was supported by NSF grants OCE-1233255 and ARC-1203506 and ONR grant N00014-17-1-2545. The authors thank W. Ermold for assistance with buoy track analysis. The ERA-I reanalysis data are available from the ECMWF. The GISTEMP data are available from the NASA Goddard Institute for Space Science. The PIOMAS and IABP data are available from the Polar Sciences Center at the University of Washington. The NASA Team sea ice data are available from the National Snow and Ice Data Center.

References

Arthun, M., Eldevik, T., Smedsrud, L. H., Skagseth, O., & Ingvaldsen, R. B. (2012). Quantifying the influence of Atlantic heat on Barents Sea ice variability and retreat. *Journal of Climate*, *25*(13), 4736–4743. https://doi.org/10.1175/jcli-d-11-00466.1

Asplin, M. G., Lukovich, J. V., & Barber, D. G. (2009). Atmospheric forcing of the Beaufort Sea ice gyre: Surface pressure climatology and sea ice motion. *Journal of Geophysical Research*, *114*, C00A06. https://doi.org/10.1029/2008JC005127

Banzon, V., Smith, T. M., Chin, T. M., Liu, C., & Hankins, W. (2016). A long-term record of blended satellite and in situ sea-surface temperature for climate monitoring, modeling and environmental studies. *Earth System Science Data*, *8*(1), 165–176. https://doi.org/10.5194/essd-8-165-2016

Batty, D. (2015). North Pole could be 35C warmer than average this week, warn meteorologists. *The Guardian*.

Blackmon, M. L., Wallace, J. M., Lau, N.-C., & Mullen, S. L. (1977). An observational study of the Northern Hemisphere wintertime circulation. *Journal of the Atmospheric Sciences*, *34*(7), 1040–1053. https://doi.org/10.1175/1520-0469(1977)034%3C1040:AOSOTN%3E2.0.CO;2

Boisvert, L. N., Petty, A. A., & Stroeve, J. C. (2016). The impact of the extreme winter 2015/16 Arctic cyclone on the Barents–Kara Seas. *Monthly Weather Review*, *144*(11), 4279–4287. https://doi.org/10.1175/MWR-D-16-0234.1

Bromwich, D. H., Wilson, A. B., Bai, L. S., Moore, G. W. K., & Bauer, P. (2016). A comparison of the regional Arctic System Reanalysis and the global ERA-Interim Reanalysis for the Arctic. *Quarterly Journal of the Royal Meteorological Society*, *142*(695), 644–658. https://doi.org/10.1002/qj.2527

Brummer, B. (1999). Roll and cell convection in wintertime arctic cold-air outbreaks. *Journal of the Atmospheric Sciences*, *56*(15), 2613–2636. https://doi.org/10.1175/1520-0469(1999)056%3C2613:racciw%3E2.0.co;2

Cavalieri, D. J., Parkinson, C. L., Gloersen, P., Comiso, J. C., & Zwally, H. J. (1999). Deriving long-term time series of sea ice cover from satellite passive-microwave multisensor data sets. *Journal of Geophysical Research*, *104*(C7), 15,803–15,814. https://doi.org/10.1029/1999JC900081

Cavallo, S. M., & Hakim, G. J. (2010). Composite structure of tropopause polar cyclones. *Monthly Weather Review*, *138*(10), 3840–3857. https://doi.org/10.1175/2010MWR3371.1

Chang, E. K. (2009). Are band-pass variance statistics useful measures of storm track activity? Re-examining storm track variability associated with the NAO using multiple storm track measures. *Climate Dynamics*, *33*(2–3), 277–296. https://doi.org/10.1007/s00382-009-0532-9

Chylek, P., Folland, C. K., Lesins, G., & Dubey, M. K. (2010). Twentieth century bipolar seesaw of the Arctic and Antarctic surface air temperatures. *Geophysical Research Letters*, *37*, L08703. https://doi.org/10.1029/2010GL042793

Cohen, J., Screen, J. A., Furtado, J. C., Barlow, M., Whittleston, D., Coumou, D., et al. (2014). Recent Arctic amplification and extreme mid-latitude weather. *Nature Geoscience*, *7*(9), 627–637. https://doi.org/10.1038/ngeo2234

Cullather, R. I., Lim, Y. K., Boisvert, L. N., Brucker, L., Lee, J. N., & Nowicki, S. M. (2016). Analysis of the warmest Arctic winter, 2015–2016. *Geophysical Research Letters*, *43*, 10,808–10,816. https://doi.org/10.1002/2016GL071228

Day, J. J., Holland, M. M., & Hodges, K. I. (2017). Seasonal differences in the response of Arctic cyclones to climate change in CESM1. *Climate Dynamics*, 1–19. https://doi.org/10.1007/s00382-017-3767-x

Dee, D. P., Uppala, S. M., Simmons, A. J., Berrisford, P., Poli, P., Kobayashi, S., et al. (2011). The ERA-Interim reanalysis: Configuration and performance of the data assimilation system. *Quarterly Journal of the Royal Meteorological Society*, *137*(656), 553–597. https://doi.org/10.1002/qj.828

Deser, C., Tomas, R. A., & Peng, S. (2007). The transient atmospheric circulation response to North Atlantic SST and sea ice anomalies. *Journal of Climate*, *20*(18), 4751–4767. https://doi.org/10.1175/JCLI4278.1

Ghil, M., Allen, M. R., Dettinger, M. D., Ide, K., Kondrashov, D., Mann, M. E., et al. (2002). Advanced spectral methods for climatic time series. *Reviews of Geophysics*, *40*(1), 1003. https://doi.org/10.1029/2000RG000092

Haine, T. W. N., Curry, B., Gerdes, R., Hansen, E., Karcher, M., Lee, C., et al. (2015). Arctic freshwater export: Status, mechanisms, and prospects. *Global and Planetary Change*, *125*, 13–35. https://doi.org/10.1016/j.gloplacha.2014.11.013

Hansen, J., Ruedy, R., Glascoe, J., & Sato, M. (1999). GISS analysis of surface temperature change. *Journal of Geophysical Research*, *104*(D24), 30,997–31,022. https://doi.org/10.1029/1999JD900835

Hansen, J., Ruedy, R., Sato, M., & Lo, K. (2010). Global surface temperature change. *Reviews of Geophysics*, *48*, RG4004. https://doi.org/10.1029/2010RG000345

Hoskins, B. J., & Hodges, K. I. (2002). New perspectives on the Northern Hemisphere winter storm tracks. *Journal of the Atmospheric Sciences*, *59*(6), 1041–1061. https://doi.org/10.1175/1520-0469(2002)059%3C1041:NPOTNH%3E2.0.CO;2

Hoskins, B. J., McIntyre, M. E., & Robertson, A. W. (1985). On the use and significance of isentropic potential vorticity maps. *Quarterly Journal of the Royal Meteorological Society*, *111*(470), 877–946. https://doi.org/10.1002/qj.49711147002

Jahnke-Bornemann, A., & Brummer, B. (2009). The Iceland-Lofotes pressure difference: Different states of the North Atlantic low-pressure zone. *Tellus Series a-Dynamic Meteorology and Oceanography*, *61*(4), 466–475. https://doi.org/10.1111/j.1600-0870.2009.00401.x

Lindsay, R. W., & Zhang, J. (2005). The thinning of Arctic sea ice, 1988–2003: Have we passed a tipping point? *Journal of Climate*, *18*(22), 4879–4894. https://doi.org/10.1175/JCLI3587.1

Lindsay, R., Wensnahan, M., Schweiger, A., & Zhang, J. (2014). Evaluation of seven different atmospheric reanalysis products in the Arctic. *Journal of Climate*, *27*(7), 2588–2606. https://doi.org/10.1175/JCLI-D-13-00014.1

Manucharyan, G. E., & Spall, M. A. (2016). Wind-driven freshwater buildup and release in the Beaufort Gyre constrained by mesoscale eddies. *Geophysical Research Letters*, *43*, 273–282. https://doi.org/10.1002/2015GL065957

McPhee, M. G. (2012). Intensification of geostrophic currents in the Canada Basin, Arctic Ocean. *Journal of Climate*, *26*(10), 3130–3138. https://doi.org/10.1175/JCLI-D-12-00289.1

Moore, G. W. K. (2016). The December 2015 North Pole warming event and the increasing occurrence of such events. *Scientific Reports*, *6*(1), 39,084. https://doi.org/10.1038/srep39084

Moore, G. W. K., Reader, M. C., York, J., & Sathiyamoorthy, S. (1996). Polar lows in the Labrador Sea. *Tellus A*, *48*(1), 17–40. https://doi.org/10.1034/j.1600-0870.1996.00002.x

Moore, G. W. K., Renfrew, I. A., & Pickart, R. S. (2012). Spatial distribution of air-sea heat fluxes over the sub-polar North Atlantic Ocean. *Geophysical Research Letters*, *39*, L18806. https://doi.org/10.1029/2012GL053097

Moore, G. W. K., Våge, K., Pickart, R. S., & Renfrew, I. A. (2015). Decreasing intensity of open-ocean convection in the Greenland and Iceland seas. *Nature Climate Change*, *5*(9), 877–882. https://doi.org/10.1038/nclimate2688

Morice, C. P., Kennedy, J. J., Rayner, N. A., & Jones, P. D. (2012). Quantifying uncertainties in global and regional temperature change using an ensemble of observational estimates: The HadCRUT4 data set. *Journal of Geophysical Research*, *117*, D08101. https://doi.org/10.1029/2011JD017187

Overland, J. E., & Wang, M. (2016). Recent extreme Arctic temperatures are due to a split polar vortex. *Journal of Climate*, *29*(15), 5609–5616. https://doi.org/10.1175/JCLI-D-16-0320.1

Parkinson, C. L., & Cavalieri, D. J. (2008). Arctic sea ice variability and trends, 1979–2006. *Journal of Geophysical Research*, *113*, C07003. https://doi.org/10.1029/2007JC004558

Petty, A. A., Hutchings, J. K., Richter-Menge, J. A., & Tschudi, M. A. (2016). Sea ice circulation around the Beaufort Gyre: The changing role of wind forcing and the sea ice state. *Journal of Geophysical Research: Oceans*, *121*, 3278–3296. https://doi.org/10.1002/2015JC010903

Petty, A. A., Stroeve, J. C., Holland, P. R., Boisvert, L. N., Bliss, A. C., Kimura, N., & Meier, W. N. (2017). The Arctic sea ice cover of 2016: A year of record low highs and higher than expected lows. *The Cryosphere Discuss*, *2017*, 1–33. https://doi.org/10.5194/tc-2017-207

Proshutinsky, A., Krishfield, R., Timmermans, M.-L., Toole, J., Carmack, E., McLaughlin, F., et al. (2009). Beaufort Gyre freshwater reservoir: State and variability from observations. *Journal of Geophysical Research*, *114*, C00A10. https://doi.org/10.1029/2008JC005104

Rigor, I. G., Wallace, J. M., & Colony, R. L. (2002). Response of sea ice to the Arctic oscillation. *Journal of Climate*, *15*(18), 2648–2663. https://doi.org/10.1175/1520-0442(2002)015%3C2648:ROSITT%3E2.0.CO;2

Schweiger, A. J., & Zhang, J. (2015). Accuracy of short-term sea ice drift forecasts using a coupled ice-ocean model. *Journal of Geophysical Research: Oceans*, *120*, 7827–7841. https://doi.org/10.1002/2015JC011273

Schweiger, A., Lindsay, R., Zhang, J., Steele, M., Stern, H., & Kwok, R. (2011). Uncertainty in modeled Arctic sea ice volume. *Journal of Geophysical Research*, *116*, C00D06. https://doi.org/10.1029/2011JC007084

Semmler, T., Jung, T., & Serrar, S. (2016). Fast atmospheric response to a sudden thinning of Arctic sea ice. *Climate Dynamics*, *46*(3-4), 1015–1025. https://doi.org/10.1007/s00382-015-2629-7

Serreze, M. C., & Barrett, A. P. (2010). Characteristics of the Beaufort Sea High. *Journal of Climate*, *24*(1), 159–182. https://doi.org/10.1175/2010JCLI3636.1

Serreze, M. C., & Barry, R. G. (2005). *The Arctic climate system*. Cambridge: Cambridge University Press. https://doi.org/10.1017/CBO9780511535888

Serreze, M. C., & Barry, R. G. (2014). *The Arctic climate system* (2nd ed.). New York: Cambridge University Press. https://doi.org/10.1017/CBO9781139583817

Serreze, M. C., Carse, F., Barry, R. G., & Rogers, J. C. (1997). Icelandic low cyclone activity: Climatological features, linkages with the NAO, and relationships with recent changes in the Northern Hemisphere circulation. *Journal of Climate*, *10*(3), 453–464. https://doi.org/10.1175/1520-0442(1997)010%3C0453:ILCACF%3E2.0.CO;2

Serreze, M., Barrett, A., Stroeve, J., Kindig, D., & Holland, M. (2009). The emergence of surface-based Arctic amplification. *The Cryosphere*, *3*(1), 11–19. https://doi.org/10.5194/tc-3-11-2009

Steele, M., Ermold, W., & Zhang, J. (2008). Arctic Ocean surface warming trends over the past 100 years. *Geophysical Research Letters*, *35*, L02614. https://doi.org/10.1029/2007GL031651

Stroeve, J. C., Serreze, M. C., Holland, M. M., Kay, J. E., Malanik, J., & Barrett, A. P. (2012). The Arctic's rapidly shrinking sea ice cover: A research synthesis. *Climatic Change*, *110*(3-4), 1005–1027. https://doi.org/10.1007/s10584-011-0101-1

Tsukernik, M., Kindig, D. N., & Serreze, M. C. (2007). Characteristics of winter cyclone activity in the northern North Atlantic: Insights from observations and regional modeling. *Journal of Geophysical Research*, *112*, D03101. https://doi.org/10.1029/2006JD007184

Walsh, J. E. (1978). Temporal and spatial scales of Arctic circulation. *Monthly Weather Review*, *106*(11), 1532–1544. https://doi.org/10.1175/1520-0493(1978)106%3C1532:tassot%3E2.0.co;2

Zhang, J., & Rothrock, D. A. (2003). Modeling global sea ice with a thickness and enthalpy distribution model in generalized curvilinear coordinates. *Monthly Weather Review*, *131*(5), 845–861. https://doi.org/10.1175/1520-0493(2003)131%3C0845:MGSIWA%3E2.0.CO;2

Zhang, J., Lindsay, R., Schweiger, A., & Rigor, I. (2012). Recent changes in the dynamic properties of declining Arctic sea ice: A model study. *Geophysical Research Letters*, *39*, L20503. https://doi.org/10.1029/2012GL053545